EPJ Web of Conferences **61**, 02003 (2013)
DOI: 10.1051/epjconf/ 20136102003

Radiation from accelerated particles in relativistic jets with shocks, shear-flow, and reconnection

K.-I. Nishikawa[1,a], P. Hardee[2], Y. Mizuno[3], I. Duţan[4], B. Zhang[5], M Medvedev[6], E.J. Choi[7], K. W. Min[7], J. Niemiec[8], Å. Nordlund[9], J. Frederiksen[9], H. Sol[10], M. Pohl[11], D. H. Hartmann[12], A. Marscher[13], and J. L. Gómez[14]

[1] *University of Alabama in Huntsville, 320 Sparkman Drive, ZP12, Huntsville, AL 35805, USA*
[2] *Department of Physics and Astronomy, The University of Alabama, Tuscaloosa, AL 35487, USA*
[3] *Institute of Astronomy, National Tsing-Hua University, Hsinchu, Taiwan 30013, Republic of China*
[4] *Institute of Space Science, Atomistilor 409, Bucharest-Magurele RO-077125, Romania*
[5] *Department of Physics, University of Nevada, Las Vegas, NV 89154, USA*
[6] *Department of Physics and Astronomy, University of Kansas, KS 66045, USA*
[7] *Korea Advanced Institute of Science and Technology, Daejeon 305-701, South Korea*
[8] *Institute of Nuclear Physics PAN, ul. Radzikowskiego 152, 31-342 Kraków, Poland*
[9] *Niels Bohr Institute, University of Copenhagen, Juliane Maries Vej 30, 2100 Copenhagen Ø, Denmark*
[10] *LUTH, Observatore de Paris-Meudon, 5 place Jules Jansen, 92195 Meudon Cedex, France*
[11] *Institute of Physics and Astronomy, University of Potsdam, Karl-Liebknecht-Strasse 24/25 14476 Potsdam-Golm, Germany*
[12] *Department of Physics and Astronomy, Clemson University, Clemson, SC 29634, USA*
[13] *Institute for Astrophysical Research, Boston University, 725 Commonwealth Ave., Boston, MA 02215, USA*
[14] *Instituto de Astrofísica de Andalucía, CSIC, Apartado 3004, 18080 Granada, Spain*

Abstract. We have investigated particle acceleration and shock structure associated with an unmagnetized relativistic jet propagating into an unmagnetized plasma for electron-positron and electron-ion plasmas. Strong magnetic fields generated in the trailing jet shock lead to transverse deflection and acceleration of the electrons. We have self-consistently calculated the radiation from the electrons accelerated in the turbulent magnetic fields for different jet Lorentz factors. We find that the synthetic spectra depend on the bulk Lorentz factor of the jet, the jet temperature, and the strength of the magnetic fields generated in the shock. We have investigated the generation of magnetic fields associated with velocity shear between an unmagnetized relativistic (core) jet and an unmagnetized sheath plasma. We discuss particle acceleration in collimation shocks for AGN jets formed by relativistic MHD simulations. Our calculated spectra should lead to a better understanding of the complex time evolution and/or spectral structure from gamma-ray bursts, relativistic jets, and supernova remnants.

1 Introduction

Kinetic simulations have focused on magnetic field generation via electromagnetic plasma instabilities in unmagnetized flows without velocity shears. Three-dimensional (3D) particle-in-cell (PIC) simulations of Weibel turbulence [26, 28] have demonstrated subequipartition magnetic field generation. We have calculated, self-consistently, the radiation from electrons accelerated in the turbulent magnetic fields beyond the standard models [25, 35, 36, 38–41]. We found that the synthetic spectra depend on the Lorentz factor of the jet, the jet's thermal temperature, and the strength of the generated magnetic fields [31, 32].

We have examined the strong magnetic fields generated by kinetic shear (Kelvin-Helmholtz) instabilities (KKHI). In particular the KKHI has been shown to lead to particle acceleration and magnetic field amplification in relativistic shear flows [2, 11, 33, 34]. It is very important to note that this DC magnetic field is not captured in MHD [42] or fluid theories because it results from intrinsically kinetic phenomena. Furthermore, since the DC field is stronger than the AC field, a kinetic treatment is clearly required in order to fully capture the field structure generated in unmagnetized or weakly magnetized relativistic flows with velocity shear. This characteristic field structure will also lead to a distinct radiation signature [4, 16, 31, 32, 37]. A shear flow upstream of a shock can lead to density inhomogeneities via the MHD Kelvin-Helmholtz instability (KHI) which may provide important scattering sites for particle acceleration.

Observations suggest that γ-ray flares are associated with a burst in particle and magnetic energy density accompanying jet disturbances when they cross the radio core. This could be explained if the radio core is associated with a recollimation shock [7, 13–15]. We have simulated collimation shocks using RAISHIN 3-D GRMHD/RMHD code [23, 24]. Some initial results are reported for the first time.

[a] e-mail: ken-ichi.nishikawa@nasa.gov

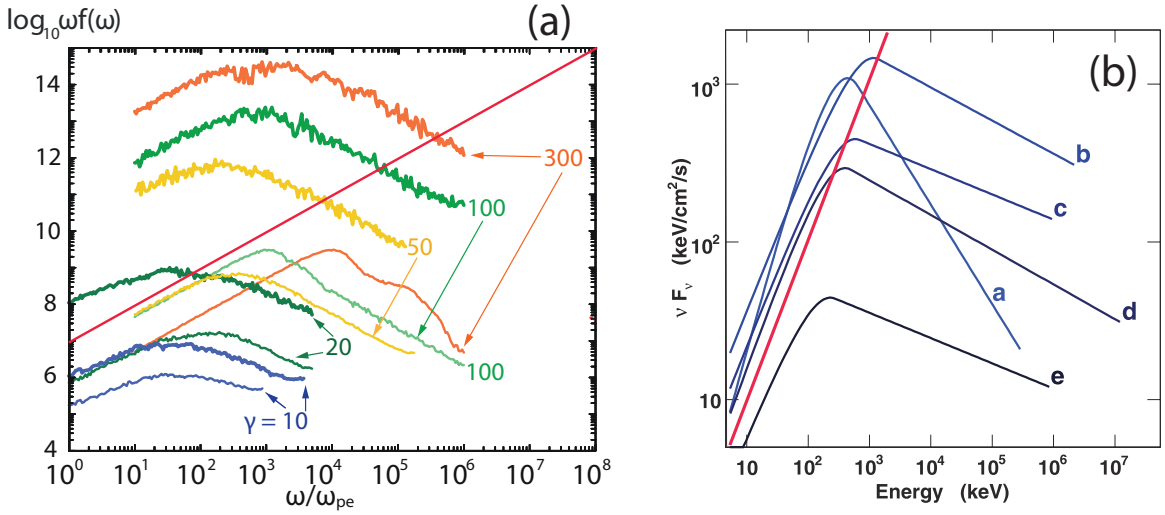

Figure 1. Figure 1a shows spectra for cold (thin lines) and warm (thick lines) electrons in jets with $\gamma = 10$, 20, 50, 100, and 300. Figure 1b shows modeled Fermi spectra in νF_ν units at early (a) to late (e) times (Abdo et al. 2009). The solid red lines indicate a slope of $\nu F_\nu = 1$

2 Self-consistent radiation calculation from PIC simulations

Electrons are accelerated in the electromagnetic fields generated by the Weibel and KKHI instabilities. Radiation can be calculated using the particle trajectories in the self-consistent turbulent magnetic fields. This calculation allows for Jitter radiation [17, 18] which is different from standard synchrotron emission. Radiation details from our simulations can be found in [31].

We have calculated the radiation spectra directly from our simulations by integrating the expression for the retarded power, derived from Liénard-Wiechert potentials for a large number of representative particles in the PIC representation of the plasma[4, 9, 10, 16, 27, 29–31, 37]. Initially we verified the technique by calculating radiation from electrons propagating in a uniform parallel magnetic field [29]. It should be noted that spectra obtained from colliding jet simulations (fixed contact discontinuity) do not provide spectra in the observer's rest frame, and cannot be compared with observed spectra [37].

The spectra shown in Figure 1a are for emission from jets with Lorentz factors $\gamma = 10$, 20, 50, 100, and 300 [31, 32]. In the figure we show two spectra for each Lorentz factor (represented by the same color line) for initially cold ($v_{\rm jet,th} = 0.01c$) (thin, lower lines) and initially warm ($v_{\rm jet,th} = 0.1c$) (thick, upper lines) jet electrons. Here the spectra are calculated for emission along the jet axis ($\theta = 0°$). The radiation shows a Bremsstrahlung-like spectrum at low frequencies for the eleven cases [9] because the magnetic fields generated by the Weibel instability are rather weak and jet electron acceleration is modest. A low frequency slope of $\nu F_\nu = 1$ is indicated by the straight red lines. The low frequency slopes in our synthetic spectra are very similar to those of the spectra in Figure 1b from [1], and show change with the Lorentz factor like the temporal evolution observed by Fermi (e.g., Fig.1b).

We have calculated radiation from accelerated electrons which are simulated using large system $8000 \times 240\times$ which will be reported separately.

3 Our Core-Sheath Jet KKHI Results

The simulation setup for our study of velocity shears (not counter-streaming shear flows as used by [2, 11] is shown in Figure 2a. In our simulation a relativistic jet plasma is surrounded by a sheath plasma [33, 34]. This setup is similar to the setup of our RMHD simulations [22]. In our initial simulation the jet core has $v_{\rm core} = 0.9978c$ ($\gamma = 15$) pointing in the positive x direction in the middle of the simulation box as in [2]. Unlike Alves et al. [2] the upper and lower quarter of the simulation box contain a stationary, $v_{\rm sheath} = 0$, sheath plasma. Our setup allows for motion of the sheath plasma in the positive x direction.

Overall, this structure is similar in spirit, although not in scale, to that proposed for active galactic nuclei (AGN) relativistic jet cores surrounded by a slower moving sheath, and is also relevant to gamma-ray burst (GRB) jets. In particular, we note that this structure is also relevant to the "jet-in-a-jet" or "needles in a jet" scenarios [5], which have been invoked to provide smaller scale high speed structures within a much larger more slowly moving AGN jet. Similar smaller scale structures within GRB jets are also conceivable.

This more realistic setup is different from the initial conditions used by the previous simulations with counter-steaming flows [2], and hence allows us to compute synthetic spectra in the observer frame. As mentioned by [2], in a non-counterstreaming or unequal density counterstreaming setup the growing KKHI will propagate with the flow. For GRB jets, the relativistic jet core will have

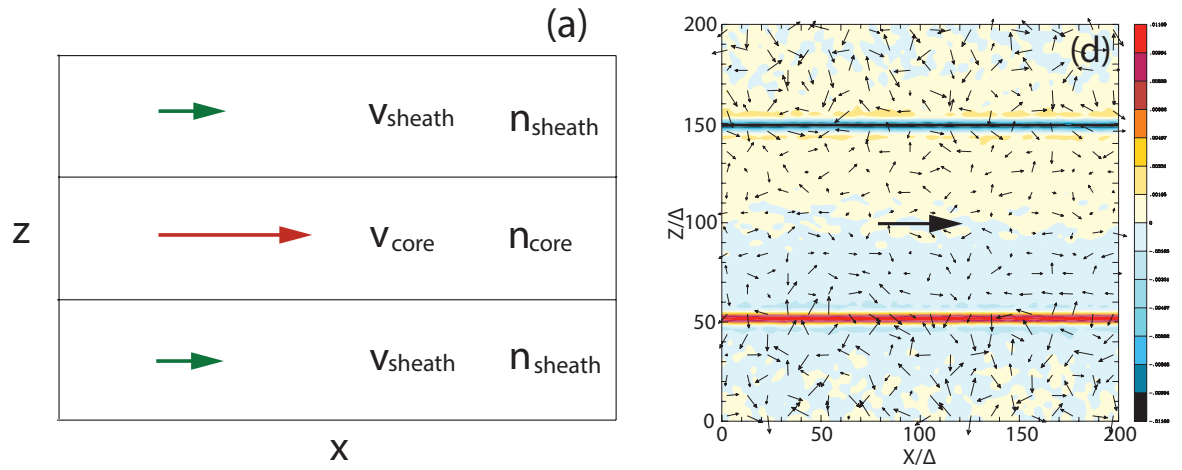

Figure 2. Figure 2a shows our simulation model where the sheath plasma can be stationary or moving in the same direction as the jet core. In this simulation the sheath velocity is zero. Figure 2b shows the magnitude of B_y is plotted in the $x-z$ plane (jet flow in the $+x$-direction indicated by the large arrow) at the center of the simulation box, $y = 100\Delta$ at simulation time $t = 70\,\omega_{pe}^{-1}$ for the case of $\gamma_j = 15$ and $m_i/m_e = 1836$. This panel covers one fifth of the whole simulation system. The arrows show the magnetic field in the plane.

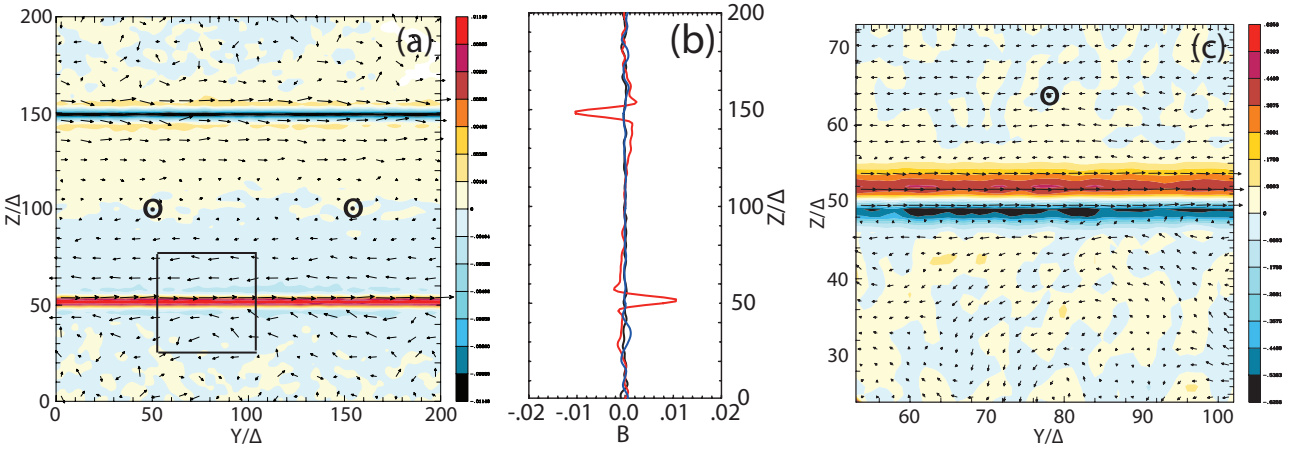

Figure 3. Magnetic field structure generated by a relativistic electron-ion jet core with $\gamma = 15$ and stationary sheath plasma at simulation time $t = 70\,\omega_{pe}^{-1}$. The magnitude of B_y is plotted (a) in the $y-z$ plane (jet flow out of the page) at the center of the simulation box, $x = 500\Delta$ at the center of the simulation box, $y = 100\Delta$. Figure 3b shows B_y (red), B_x (black), and B_z (blue) at $x = 500\Delta$ and $y = 100\Delta$. Figure 3c shows the x component of the electric current (jet flow is out of the page) in the region indicated the square box in Fig. 3a. The current is positive on the core side and negative on the sheath side of the velocity shear. The positive current is stronger than the negative current, leading to B_y as shown in Figure 3b. The small arrows show the magnetic field in the plane.

much higher density relative to the external medium. On the other hand, for an AGN jet the relativistic core is less dense than the surrounding sheath.

We previously reported results from our first simulations for a core-sheath case with $\gamma_j = 15$ and $m_i/m_e = 20$ [33]. We have also reported simulation results using the real mass ratio $m_i/m_e = 1836$[33]. We find some differences from previous counter-streaming cases.

We have performed a simulation using a system with $(L_x, L_y, L_z) = (1005\Delta, 205\Delta, 205\Delta)$ and with an ion to electron mass ratio of $m_i/m_e = 1836$ ($\Delta = 1$ is the system size). The jet and sheath plasma density is $n_{jt} = n_{am} = 8$. The electron skin depth, $\lambda_s = c/\omega_{pe} = 12.2\Delta$, where $\omega_{pe} = (e^2 n_a/\epsilon_0 m_e)^{1/2}$ is the electron plasma frequency and the electron Debye length λ_D is 1.2Δ. The jet Lorentz factor is $\gamma_j = 15$. The jet-electron thermal velocity is $v_{j,th,e} = 0.014\,c$ in the jet reference frame, where c is the speed of light. The electron/ion thermal velocity in the ambient plasma is $v_{a,th,e} = 0.03\,c$. Ion thermal velocities are smaller by $(m_i/m_e)^{1/2}$. We use periodic boundary conditions on all boundaries [3, 28]

Figure 2b shows the magnitude of B_y plotted in the $x-z$ plane (jet flow in the $+x$-direction indicated by the large arrow) at the center of the simulation box, $y = 100\Delta$ at

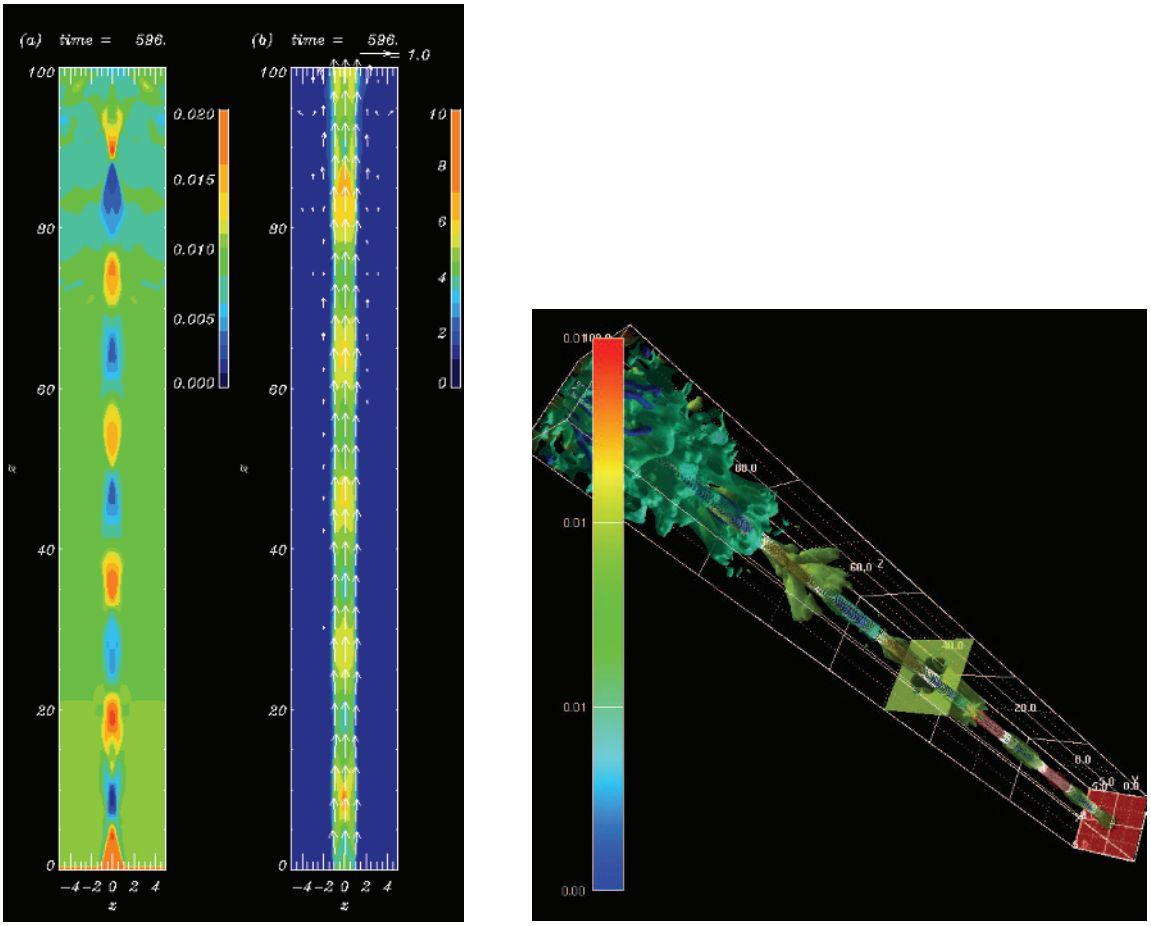

Figure 4. Figure 4show the collimation shocks at $t = 600R_j/c$ in 2-D (left panel) and 3-D (right panel) with $\eta = \rho_j/\rho_a = 10^{-3}, \gamma_j = 4, \mathcal{M} = 1.69, R_j = 1.0$. The left column shows gas pressure (left) and Lorentz factor (right) with velocity vector on xz-plane at $y = 0$.

simulation time $t = 70\,\omega_{pe}^{-1}$. The arrows show the magnetic field $B_{x,z}$ in the plane.

Figure 3 shows the magnetic field structures generated by the relativistic electron-ion core with $\gamma = 15$ and with a stationary sheath plasma at time $t = 70\,\omega_{pe}^{-1}$. Figure 3a shows the magnitude of B_y plotted in the $y - z$ plane (jet flow is out of the page) at the center of the simulation box, $x = 500\Delta$. Figure 3b shows B_y (red), B_x (black), and B_z (blue) magnetic field components at $x = 500\Delta$ and $y = 100\Delta$. Figure 3c shows the x component of the current in the region indicated by the square box in Fig. 3a. Relativistic jet flow is out of the page and positive (red) current flows along the jet side, whereas negative (blue) current flows along the sheath side. Positive currents are stronger than the negative currents, leading to B_y as shown in Figs. 3a and 2b.

We have compared the differences between cases with mass ratios $m_i/m_e = 20$ and 1836 for the relativistic jet with $\gamma_j = 15$. We find that the structure and growth rate of kinetic KHI is very similar [34]. The heavier ions in the real mass ratio case keep the system thermal fluctuations smaller, but the kinetic KHI grows similarly. The magnetic field energy becomes larger than the electric field energy at a similar time in both cases around $t = 87\,\omega_{pe}^{-1}$. We also performed a simulation with $\gamma_j = 1.5$ and $m_i/m_e = 20$. For this non-relativistic case the magnetic field grows earlier and overtakes the electric field energy at $t = 46\,\omega_{pe}^{-1}$, which is much earlier than those in the relativistic cases [34].

In forthcoming work we will obtain synthetic spectra from particles accelerated by KKHI as we have done for shock simulations [31, 32]. Electrons which are drifting the regions where the strong DC magnetic fields are generated may radiate in a different way. Ultimately we need to simulate a relativistic jet injected in an ambient plasma where shocks and KKHI are simultaneously investigated.

4 RMHD Simulations of Recollimation Shocks

Both moving "internal" shocks and standing "external" shocks can occur in a relativistic jet. The former are driven by velocity and/or pressure fluctuations in the injected flow. External shocks result from non-linear instabilities, including pressure mismatches with the external medium that cause quasi-periodic collimation/decollimation shocks and rarefactions to form.

To obtain a better understanding of the jet dynamics associated with relativistic shocks we have started to per-

form relativistic magnetohydrodynamical (RMHD) simulations using the RAISHI code [23, 24]. In order to obtain a series of strong recollimation shocks, we assume that external gas pressure decreases with axial distance. The lighter jet with weak helical magnetic field is continuously injected from inner boundary with pressure matched with external medium. The simulations are performed in 3-D cartesian coordinates. The simulation size is $-5R_{\rm j} < x, y < 5R_{\rm j}$, $0 < z < 100R_{\rm j}$ with $80 \times 80 \times 800$ grids. Figure 4 (left panel) shows the gas pressure (left) and Lorentz factor (right) with velocity vector on xz-plane at $y = 0$ at $t = 600R_{\rm j}/c$. The preliminary simulation shows the propagating jet is accelerated and over-pressured against external medium due to the decreasing external medium. In long-term evolution, the multiple recollimation shock structure is developed. The jet Lorentz factor is correlated with the recollimation shock structure. The higher gas pressure region has lower jet velocity and lower gas pressure region has higher jet velocity.

Using the magnetohydrodynamical results as input, synchrotron emission is then computed at different observing frequencies [6, 7, 21]. Analysis of the core position in the simulated emission maps reveals the expected behavior in case the VLBI core corresponds to a recollimation shock, as the multi-wavelength analysis of γ-ray flares in blazar suggests.

The "Turbulent Extreme Multi-Zon" (TEMZ) code is developed by Marscher [12], calculates the spectral energy distribution (multi-wavelength light curves) from synchrotron radiation and inverse Compton scattering, as well as the linear polarization of the synchrotron emission at various frequencies, as a function of both time and location within the jet. The RMHD simulation results will provide necessary information for this calculation by TEMZ. In the current version of the code, a standing conical collimation shock energizes electrons in the turbulent plasma. The energy density at the jet input varies with time stochastically within a power-law power spectrum with slope similar to that observed for flux variations. The magnetic field direction varies randomly from one cell of plasma to the next. Further development, in addition to parallelization of the code to run on a high-energy computer, is needed to include (1) shocks and rarefactions that are more realistic, as generated by the proposed RMHD simulations; (2) moving shocks, which are not currently incorporated; (3) dynamically generated rather than randomly assigned turbulent magnetic field and velocity fluctuations, as produced by the simulations proposed here; and (4) nonthermal seed photons from the many (essentially co-moving) cells, a slower moving sheath, and emission-line clouds near the jet. More generally, we will continue to investigate the possibility that γ-rays flares in AGN jets can be produced by the interaction of moving shocks with standing recollimation shocks.

5 Summary and Discussion

We have investigated generation of magnetic fields associated with velocity shear between an unmagnetized relativistic jet and an unmagnetized sheath plasma (core jet-sheath configuration). We have examined the evolution of electric and magnetic fields generated by kinetic shear (Kelvin-Helmholtz) instabilities. Compared to the previous studies using counter-streaming performed by Alves et al. (2012) [2], the structure of KKHI of our jet-sheath configuration is slightly different even for the global evolution of the strong transverse magnetic field. We find that the major components of growing modes are $E_{\rm z}$ and $B_{\rm y}$. After the $B_{\rm y}$ component is excited, the induced electric field $E_{\rm x}$ becomes larger. However, other components are very small. We find that the structure and growth rate with electron KKHI with the cases to the real mass ration $m_{\rm i}/m_{\rm e} = 1836$ and $m_{\rm i}/m_{\rm e} = 20$ are similar. In our simulations with jet-sheath case no saturation at the later time is seen as in the counter-streaming cases. This difference seems come from that fact that the jet is highly relativistic and our simulation is done in jet-sheath configuration. The growth rate with mildly-relativistic jet case ($\gamma_{\rm j} = 1.5$) is larger than the relativistic jet case ($\gamma_{\rm j} = 15$).

We have extended the analysis presented in [8] to core-sheath electron-proton plasma flows allowing for different core and sheath electron densities $n_{\rm jt}$ and $n_{\rm am}$, respectively, and core and sheath electron velocities $v_{\rm jt}$ and $v_{\rm am}$, respectively. In this analysis the protons are considered to be free-streaming whereas the electron fluid quantities and fields are linearly perturbed. We consider electrostatic modes along the jet. The dispersion relation becomes:

$$\begin{aligned}
&(k^2c^2 + \gamma_{\rm am}^2\omega_{\rm p,am}^2 - \omega^2)^{1/2}(\omega - kV_{\rm am})^2 \\
&\times[(\omega - kV_{\rm jt})^2 - \omega_{\rm p,jt}^2] \\
&+(k^2c^2 + \gamma_{\rm jt}^2\omega_{\rm p,jt}^2 - \omega^2)^{1/2}(\omega - kV_{\rm jt})^2 \\
&\times[(\omega - kV_{\rm am})^2 - \omega_{\rm p,am}^2] = 0, \qquad (1)
\end{aligned}$$

where $\omega_{\rm p,jt}$ and $\omega_{\rm p,am}$ are the plasma frequencies ($\omega_{\rm p}^2 \equiv 4\pi ne^2/\gamma^3 m_{\rm e}$) of jet and ambient electrons, respectively, $k = k_{\rm x}$ is the wave number parallel to the jet flow, and $\gamma_{\rm jt}$ and $\gamma_{\rm am}$ are Lorentz factors of jet and ambient electrons, respectively. Some analytical and numerical results are described in the previous reports [33, 34].

We have calculated, self-consistently, the radiation from electrons accelerated in the turbulent magnetic fields in the relativistic shocks. We found that the synthetic spectra depend on the Lorentz factor of the jet, the jet's thermal temperature, and the strength of the generated magnetic fields [31, 32]. In forthcoming work we will obtain synthetic spectra from particles accelerated by KKHI as we have done for shock simulations [31, 32].

The initial simulation results with recollimation shocks encourage us to more simulations and prepare next steps to calculate emission and calculate particle acceleration using relativistic Monte Carlo based on the realistic recollimation shock structures [19, 20].

Acknowledgements

This work is supported by NSF AST-0908010, and AST-0908040, NASA NNX09AD16G, NNX12AH06G, NNX13AP14G and NNX13AP21G. JN is supported by

NCN through grant DEC-2011/01/B/ST9/03183 and DEC-2012/04/A/ST9/00083. YM is supported by the Taiwan National Science Council under the grant NSC 100-2112-M-007-022-MY3. Simulations were performed at the Columbia and Pleiades facilities at the NASA Advanced Supercomputing (NAS) and Kraken and Nautilus at The National Institute for Computational Sciences (NICS) which is supported by the NSF. This research was started during the program "Chirps, Mergers and Explosions: The Final Moments of Coalescing Compact Binaries" at the Kavli Institute for Theoretical Physics which is supported by the National Science Foundation under Grant No. PHY05-51164.

References

[1] Abdo, A. A., et al., Science **323**, 1688 (2009)

[2] Alves, E. P. et al. ApJ **746**, L14 (2012)

[3] Buneman, O., *Computer Space Plasma Physics: Simulation Techniques and Software* (Terra Scientific Publishing Company, Tokyo, Japan, 1993) 67

[4] Frederiksen, J. T., Haugbølle, T., Medvedev, M. V., & Nordlund, Å., ApJ **722**, L114 (2010)

[5] Giannios, D., Uzdensky, D. A. and Begelman, M. C., MNRAS **395**, L29 (2009)

[6] Gómez, J. L., Martí, J. M., Marscher, A. P., Ibánez, J. M. & Marcaide, J. M., ApJ, **449**, L19 (1995)

[7] Gómez, J. L., Martí, J. M., Marscher, A. P., Ibáñez, J. M., & Alberdi, A., ApJ **482**, L33 (1997)

[8] Gruzinov, A. 2008, arXiv:0803.1182

[9] Hededal, C.B., *Gamma-Ray Bursts, Collisionless Shocks and Synthetic Spectra*, Ph.D. thesis, (2005) (arXiv:astro-ph/0506559)

[10] Jackson, J. D., *Classical Electrodynamics*, Interscience, (1999)

[11] Liang, E., Boettcher, M., & Smith, I., ApJ **766**, L19 (2013)

[12] Marscher, A. P., 2012 Fermi Symposium proceedings –eConf C121028, arXiv:1304.2064 (2013)

[13] Marscher, A. P., ASP Conference Series **402**, 194 (2009)

[14] Marscher, A. P., et al., Nature, **452**, 966 (2008)

[15] Marscher, A. P., et al. , ApJ, **710**, L126 (2010)

[16] Martins, J.L., Martins, S.F., Fonseca R.A., & Silva, L.O., Proc. of SPIE, **7359**, 73590V-1–8 (2009)

[17] Medvedev, M. V., ApJ **540**, 704 (2000)

[18] Medvedev, M. V., ApJ **637**, 869 (2006)

[19] Meli, A., Astroph. Space Sci. Trans. **7**, 287 (2011)

[20] Meli, A., & Biermann, P. L., A&A, **556**, A88 (2013)

[21] Mimica, P., Aloy, M.-A., Martí, J. M., Gómez, J. L., & Miralles, J. A., ApJ **696**, 1142 (2009)

[22] Mizuno, Y., Hardee, P. and Nishikawa, K.-I., ApJ **662**, 835 (2007)

[23] Mizuno, Y., Hardee, P. and Nishikawa, K.-I., ApJ **734**, 19 (2011)

[24] Mizuno, Y., Nishikawa, K.-I., Koide, S., Hardee, P., & Fishman, G. J., preprint, arXiv:astro-ph/0609004, (2006)

[25] Nakar, E., Physics Reports **442**, 166 (2007)

[26] Nishikawa, K.-I., Hardee, P., Richardson, G., Preece, R., Sol, H., & Fishman, G. J., ApJ **622**, 927 (2005)

[27] Nishikawa, K.-I., Mizuno, Y., Fishman, G.J., & Hardee, P., IJMPD **17**, 1761 (2008)

[28] Nishikawa, K.-I., Niemiec, J., Hardee, P. Medvedev, M., Sol, H., Mizuno, Y., Zhang, B., Pohl, M., Oka, M., & Hartmann, D. H., ApJ **698**, L10 (2009a)

[29] Nishikawa, K. -I., Niemiec, J., Sol, H., Medvedev, M., Zhang, B., Nordlund, Å., Frederiksen, J. T., Hardee, P., Mizuno, Y., Hartmann, D. H., & Fishman, G. J., AIPCP **1085**, 589 (2009b)

[30] Nishikawa, K.-I., Niemiec, J., Medvedev, M., Zhang, B., Hardee, P., Mizuno, Y., Nordlund, Å. Frederiksen, J., Sol, H., Pohl, M., Hartmann, D. H., Oka, M., & Fishman, J. F., IJMPD **19**, 715 (2010)

[31] Nishikawa, K.-I., Niemiec, J., Medvedev, M., Zhang, B., Hardee, P., Nordlund, Å. Frederiksen, J., Mizuno, Y., Sol, H., Pohl, M., Hartmann, D. H., Oka, M., & Fishman, J. F., Adv. in Spa Res. **47**, 1434 (2011)

[32] Nishikawa, K.-I., Niemiec, J., Zhang, B., Medvedev, M., Hardee, P., Mizuno, Y., Nordlund, Å. Frederiksen, J., Sol, H., Pohl, M., Hartmann, D. H., & Fishman, J. F., IJMP: Conference Series **8**, 259 (2012)

[33] Nishikawa, K.-I., Hardee, P., Zhang, B., Dutan, I., Medvedev, M., Choi, E. J., Min, K. W., Niemiec, J., Mizuno, Y., Nordlund, Å. Frederiksen, J., Sol, H., Pohl, M., and Hartmann, D. H., 2012 Fermi Symposium proceedings –eConf C121028, arXiv:1303.2569 (2013)

[34] Nishikawa, K.-I., Zhang, B., Dutan, I., Medvedev, M., Hardee, P., Choi, E.-J., Min, K., Niemiec, J., Mizuno, Y., Nordlund, Å., Frederiksen, J., Sol, H., Pohl, M., Hartmann, D. H., Ann. Geophys., **31** 1535-1541 (2013)

[35] Panaitescu, A., Kumar, P., ApJ **560**, L49 (2001)

[36] Piran, T., AIPC **797**, 123 (2005)

[37] Sironi, L., & Spitkovsky, A., ApJ **707**, L92 (2009)

[38] Waxman, E., Plasma Phys. Control. Fusion, **48**, B137 (2006)

[39] Yost, S. A., Harrison, F. A., Sari, R., Frail, D. A., ApJ **597**, 459 (2003)

[40] Zhang, B. & Meszaros, P., IJMP A **19**, 2385 (2004)

[41] Zhang, B., AIPC, **921**, 261 (2007)

[42] Zhang, W., MacFadyen, A., & Wang, P., ApJ, **692**, L40 (2009)